Electron−Phonon Interactions and Jahn−Teller Effects in the Monocation of Corannulene

Takashi Kato* and Tokio Yamabe

Institute for Innovative Science and Technology, Graduate School of Engineering, Nagasaki Institute of Applied Science, 3-1, Shuku-machi, Nagasaki 851-0121, Japan

Received: June 21, 2005

Electron−phonon interactions in the monocation of corannulene are studied by using the hybrid Hartree−Fock (HF)/density-functional-theory (DFT) method in the Gaussian 98 program package. The C−C stretching mode of 1498 cm^{-1} most strongly couples to the e_1 highest occupied molecular orbitals (HOMO) in corannulene. The total electron−phonon coupling constant for the monocation (l_{HOMO}) of corannulene is estimated to be 0.165 eV. The l_{HOMO} value for corannulene is much larger than those for coronene and acenes with similar numbers of carbon atoms. The delocalized electronic structures and the intermediate characteristics between the strong σ-orbital interactions and weak π-orbital interactions originating from a bowl-shaped C_{5v} geometry are the main reason that the l_{HOMO} value for corannulene is much larger than those for planar D_{6h} symmetric π-conjugated coronene and D_{2h} symmetric π-conjugated acenes with similar numbers of carbon atoms. The electron transfer in the positively charged corannulene is also discussed. Intramolecular electron mobility ($\sigma_{intra,monocation}$) in the positively charged corannulene is estimated to be smaller than those for the positively charged π-conjugated acenes and coronene. The reorganization energy for the positively charged corannulene (0.060 eV) is estimated to be larger than those for the positively charged acenes and coronene. The strong orbital interactions between two neighboring carbon atoms in the HOMO of corannulene with the bowl-shaped structure are the main reasons for the calculated results. Thus, the larger overlap integral between two neighboring molecules is needed for the positively charged corannulene to become a better conductor than those for positively charged coronene and acenes. The smaller density of states at the Fermi level $n(0)$ values are enough for the conditions of the attractive electron−electron interactions to be realized in the monocation of corannulene than in the monocations of coronene and acenes with similar numbers of carbon atoms. The multimode problem is also treated in order to investigate how consideration of the multimode problem is closely related to the characteristics of the electron−phonon interactions.

Introduction

The Jahn−Teller theorem tells us[1] how spontaneous symmetry-breaking distortions in degenerate electronic states of nonlinear molecules will occur. Analysis of vibronic interaction[1−3] is important for the prediction of electronic control of nuclear motions in degenerate electronic systems. Application of vibronic interaction theory covers a large variety of research fields such as spectroscopy,[4] instability of molecular structure, electrical conductivity,[5] and superconductivity.[5−9] Vibronic interactions in discrete molecules can be viewed as the coupling between frontier orbitals and molecular vibrations, whereas those in solids are the coupling between free electrons near the Fermi level and acoustic phonons. There is a close analogy between them.

Barth and Lawton reported the first synthesis of corannulene $C_{20}H_{10}$ in 1966.[10] Immediately after the synthesis, molecular orbital calculations were applied to the corannulene system.[11] It was confirmed from an X-ray diffraction measurement that this molecule has a bowl-shaped structure with C_{5v} symmetry and that the five six-membered rings in the periphery are significantly out of plane.[12] After the development of new synthetic strategies,[13] many researchers have studied this bowl-shaped hydrocarbon extensively, taking cognizance of the C_{60} fullerene.[14,15] Unique structural and electronic properties in this molecule have been characterized recently.[13−18]

One of the reasons that many researchers have had special interest in bowl-shaped carbon materials is, of course, because of the brilliant discovery of the superconductivity in the alkali-doped A_3C_{60} complexes,[19] which was later found to exhibit high superconductive transition temperatures (T_c values) of more than 30 K[20] and of 40 K under pressure.[21] A large amount of theoretical work on the vibronic coupling of the fullerene complex was carried out to account for the interesting superconductive phenomena of the A_3C_{60} complexes.[22] Because of the highly symmetric structure with I_h symmetry, certain Jahn−Teller distortions are expected to occur in order to lift the degeneracy of the threefold degenerate lowest unoccupied molecular orbital (LUMO). Because corannulene has a highly symmetric C_{5v} structure, it has the twofold degenerate highest occupied molecular orbital (HOMO) and the twofold degenerate LUMO, both having an e_1 label of symmetry. We therefore expect that similar Jahn−Teller distortions should occur in positively charged corannulene.

In the previous work, we have analyzed the vibronic interactions and estimated possible T_c values in the monocations of acenes on the basis of the hypothesis that the vibronic interactions between the intramolecular vibrations and the HOMO play an essential role in the occurrence of possible superconductivity in the positively charged nanosized molecular systems.[23] Recently, on the basis of an experimental study of ionization spectra using high-resolution gas-phase photoelectron spectroscopy, the electron−phonon interactions in the positively charged acenes were well studied.[24] It was shown by the

* To whom correspondence should be addressed. E-mail: kato@cc.nias.ac.jp.

10.1021/jp0581936 CCC: $33.50
Published on Web 02/03/2006

experimental results that our predicted frequencies for the vibrational modes playing an essential role in the electron−phonon interactions[23] as well as the predicted total electron−phonon coupling constants[23] are in excellent agreement with those obtained from experimental research.[24]

The purpose of this paper is to discuss the electron−phonon interactions in the monocation of corannulene and to compare the calculated results of the monocation of corannulene with those for the monocations of π-conjugated hydrocarbons,[23] acenes such as benzene C_6H_6 (**1a**), naphthalene $C_{10}H_8$ (**2a**), anthracene $C_{14}H_{10}$ (**3a**), tetracene $C_{18}H_{12}$ (**4a**), pentacene $C_{22}H_{14}$ (**5a**), and coronene with planar structure in order to investigate how the properties of the electron−phonon interactions are closely related to the bowl-shaped structure of corannulene. We will also discuss the intramolecular electron mobility and the single charge transfer through the molecule. We estimate the reorganization energy for elementary charge transfer. In terms of the electron−phonon interactions and the reorganization energies, we discuss the relationships between the normal metallic states and superconductivity. We will discuss the conditions under which the attractive electron−electron interactions are realized in the monocation of corannulene.

Theoretical Background

Vibronic Coupling Constants. We discuss a theoretical background for the orbital vibronic coupling constants[1] in corannulene with C_{5v} geometry. Frontier orbitals and selected vibronically active modes in corannulene are shown in Figure 1. Here, we take a one-electron approximation into account; the vibronic coupling constant of the vibrational modes to the electronic states in the monocation of corannulene is defined as a sum of orbital vibronic coupling constants from all of the occupied orbitals, i,[1a]

$$g_{\text{electronic state}}(\omega_m) = \sum_{i}^{\text{occupied}} g_i(\omega_{\text{m}}) \tag{1}$$

Considering the one-electron approximation and that the first-order derivatives of the total energy vanish in the ground state at the equilibrium C_{5v} structure in neutral corannulene ($g_{\text{neutral}}(\omega_m) = \sum_i^{\text{HOMO}} g_i(\omega_m) = 0$), and an electron is partially occupied in the e_1 HOMO in the monocation, the vibronic coupling constants of the vibronically active modes to the electronic states of the monocation of corannulene can be defined by

$$g_{\text{monocation}}(\omega_m) = g_{e_1\text{HOMO}}(\omega_m) \tag{2}$$

We focus upon the diagonal processes; only the electronic states that belong to the same irreducible representations are considered. Thus, the symmetry of the vibronically active modes can be defined from the direct product of the orbital symmetries as follows:

$$e_1 \times e_1 = A_1 + A_2 + E_2 \tag{3}$$

The numbers of the vibronically active A_1 and E_2 vibrational modes in the monocation of corannulene are 9 and 18, respectively. In such a case, we must consider multimode problems; however, in the limit of linear vibronic coupling one can treat each set of modes (i.e., each mode index m) independently.[1a,23]

Let us look into vibronic coupling of the E_2 modes to the e_1 HOMO. The dimensionless orbital vibronic coupling constant

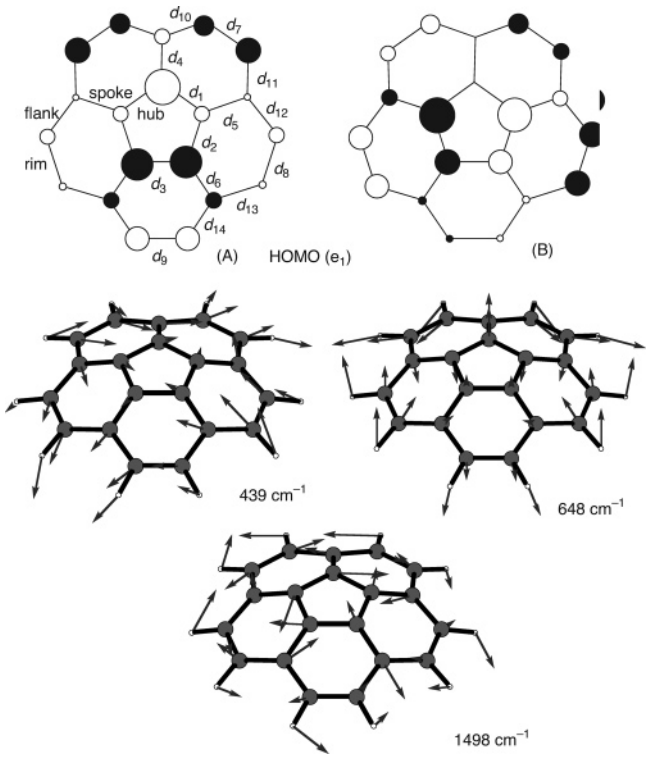

Figure 1. Phase patterns of the HOMO and selected vibronically active modes in corannulene. The optimized structures of corannulene$^+{}_{\text{A}}$ and corannulene$^+{}_{\text{B}}$ in Table 4 are obtained when the HOMO (A) and HOMO (B) are partially occupied by an electron, respectively.

of the mth mode in corannulene is defined by

$$g_{e_1\text{HOMO}}(\omega_m) = \frac{1}{\hbar\omega_m}\left\langle e_1\text{HOMO}\left|\left|\left(\frac{\partial h_{E_2m}}{\partial q_{E_2m}}\right)_0\right|\right|e_1\text{HOMO}\right\rangle \quad (m = 1, 2, ..., 18) \tag{4}$$

where q_{E_2m} is the dimensionless normal coordinate[25] of the mth vibrational mode and h_{E_2m} is the vibronic coupling matrix of the mth E_2 mode in corannulene defined as

$$h_{E_2m} = A_m\begin{pmatrix} -Q_{E_2\theta m} & Q_{E_2\epsilon m} \\ Q_{E_2\epsilon m} & Q_{E_2\theta m} \end{pmatrix} \quad (m = 1, 2, ..., 18) \tag{5}$$

Here, A_m is the reduced matrix element and the slope in the original point (i.e., $Q_{E_2\epsilon m} = Q_{E_2\theta m} = 0$) on the energy sheet of the HOMO. This is defined as

$$A_m = \left\langle e_1\text{HOMO}\left|\left|\left(\frac{\partial h_{E_2m}}{\partial Q_{E_2m}}\right)_0\right|\right|e_1\text{HOMO}\right\rangle \quad (m = 1, 2, ..., 18) \tag{6}$$

In a similar way, the dimensionless orbital vibronic coupling constant of the mth A_1 mode in corannulene is defined by

$$g_{e_1\text{HOMO}}(\omega_m) = \frac{1}{\hbar\omega_m}\left\langle e_1\text{HOMO}\left|\left|\left(\frac{\partial h_{A_1m}}{\partial q_{A_1m}}\right)0\right|\right|e_1\text{HOMO}\right\rangle \quad (m = 19, 20, ..., 27) \tag{7}$$

$$h_{A_1m} = B_m\begin{pmatrix} Q_{A_1m} & 0 \\ 0 & Q_{A_1m} \end{pmatrix} \quad (m = 19, 20, ..., 27) \tag{8}$$

$$B_m = \left\langle e_1\text{HOMO}\left|\left|\left(\frac{\partial h_{A_1m}}{\partial Q_{A_1m}}\right)_0\right|\right|e_1\text{HOMO}\right\rangle \quad (m = 19, 20, ..., 27) \tag{9}$$

TABLE 1: Reduced Masses, Vibronic Coupling Constants, and Electron−Phonon Coupling Constants (eV) for the Monocation of Corannulene

	E_2 (142)	E_2 (282)	E_2 (439)	E_2 (548)	E_2 (613)	E_2 (648)	E_2 (773)	E_2 (813)	E_2 (970)
red. masses	4.43	4.33	7.89	4.26	4.81	6.17	1.35	7.65	1.30
$g_{\mathrm{HOMO}}(\omega_m)$	0.640	0.359	0.720	0.069	0.169	0.463	0.205	0.150	0.017
$l_{\mathrm{HOMO}}(\omega_m)$	0.007	0.005	0.028	0.000	0.002	0.017	0.004	0.002	0.000

E_2 (1092)	E_2 (1172)	E_2 (1197)	E_2 (1392)	E_2 (1441)	E_2 (1498)	E_2 (1669)	E_2 (3176)	E_2 (3192)	A_1 (142)
4.75	1.49	3.29	3.95	1.65	7.31	9.52	1.09	1.09	4.60
0.269	0.105	0.068	0.157	0.070	0.537	0.056	0.004	0.003	0.226
0.010	0.002	0.001	0.004	0.001	0.054	0.001	0.000	0.000	0.000

A_1 (560)	A_1 (605)	A_1 (857)	A_1 (1052)	A_1 (1270)	A_1 (1481)	A_1 (1672)	A_1 (3195)	total
3.91	5.48	1.65	2.50	1.80	6.22	6.86	1.09	
0.232	0.001	0.122	0.212	0.334	0.365	0.009	0.069	
0.001	0.000	0.001	0.003	0.009	0.012	0.000	0.001	0.165

Electron−Phonon Coupling Constants. In the previous section, the vibronic interactions in free corannulene were described. We set up an assumption to apply the calculated vibronic coupling constants to the solid-state properties of corannulene. We assume that the conduction band of monocation crystals of corannulene consists of the HOMOs. Electron−phonon coupling constants of the E_2 modes in the monocation of corannulene are defined as follows:

$$l_{e_1\mathrm{HOMO}}(\omega_m) = g^2_{e_1\mathrm{HOMO}}(\omega_m)\hbar\omega_m \quad (m = 1, 2, ..., 18) \quad (10)$$

Those of the A_1 modes are defined as

$$l_{e_1\mathrm{HOMO}}(\omega_m) = \frac{1}{2}g^2_{e_1\mathrm{HOMO}}(\omega_m)\hbar\omega_m \quad (m = 19, 20, ..., 27) \quad (11)$$

Electron−Phonon Interactions

Electron−Phonon Coupling Constants. We performed vibrational calculations of corannulene with quadratic force constants, the second-order derivatives of the potential energy with respect to mass-weighted Cartesian displacements. In the calculation, we used the hybrid Hartree−Fock (HF)/density-functional-theory (DFT) method of Becke[26] and Lee, Yang, and Parr[27] (B3LYP), and the 6-31G* basis set.[28] The GAUSSIAN 98 program package[29] was used for our theoretical analysis. We next calculated the first-order derivatives at this equilibrium structure on each orbital energy surface by distorting the molecules along the normal coordinates of the vibronically active modes. What we obtained from the first-order derivatives is the dimensionless diagonal linear orbital vibronic coupling constants defined by eqs 4−9. We can estimate the electron−phonon coupling constants from the orbital vibronic coupling constants by using eqs 10 and 11. The orbital vibronic coupling constants estimated from analytic first-order derivatives of the energy levels of the HOMO together with reduced masses of the E_2 and A_1 modes in the neutral molecule, and electron−phonon coupling constants in the monocation of corannulene, are listed in Table 1.

We can see from Table 1 that the E_2 mode of 1498 cm^{-1} most strongly couples to the e_1 HOMO in corannulene. This can be understood as follows. When corannulene is distorted along the E_2 mode of 1498 cm^{-1}, the bonding interactions between two neighboring carbon atoms in the HOMO (A) (HOMO (B)) become weaker (stronger) and the antibonding interactions between two neighboring carbon atoms in the HOMO (A) (HOMO (B)) become stronger (weaker). Therefore, the HOMO (A) (HOMO (B)) is significantly destabilized (stabilized) in energy by such a distortion in corannulene. It should be noted that electron density on carbon atoms forming an inner ring (hub moiety) is higher than that on carbon atoms forming an outer ring in the HOMO of corannulene, and thus the orbital interactions between two neighboring carbon atoms in the hub moiety play an essential role in the electron−phonon interactions in the monocation of corannulene. And the displacements of carbon atoms in the hub moiety are large in the E_2 mode of 1498 cm^{-1}. This is the reason that the E_2 mode of 1498 cm^{-1} most strongly couples to the e_1 HOMO in corannulene. In addition to this E_2 mode, the low-frequency E_2 modes of 439 and 648 cm^{-1} also strongly couple to the e_1 HOMO in corannulene. In these modes, the reduced masses are large, and thus the displacements of carbon atoms are large. It is rational that the frequency modes in which the displacements of carbon atoms are large can strongly couple to the orbitals in which the orbital interactions between two neighboring carbon atoms are strong. This is the reason that the E_2 modes of 439 and 648 cm^{-1} as well as that of 1498 cm^{-1} afford large electron−phonon coupling constants in the monocation of corannulene. The C−C stretching A_1 mode of 1481 cm^{-1} somewhat strongly couples to the e_1 HOMO in corannulene. However, it should be noted that the A_1 modes much less strongly couple to the e_1 HOMO than the E_2 modes in corannulene.

Total Electron−Phonon Coupling Constants. Let us next look into the total electron−phonon coupling constants (l_{total}) for the monocation of corannulene. Because the l_{total} is the sum of the electron−phonon coupling constants originating from both intramolecular vibrations (l_{intra}) and intermolecular vibrations (l_{inter}), l_{total} is defined as

$$l_{\mathrm{total}} = l_{\mathrm{intra}} + l_{\mathrm{inter}} \quad (12)$$

However, it should be noted that the intramolecular orbital interactions are much stronger than the intermolecular orbital interactions. Therefore, it is rational that the l_{intra} values are much larger than the l_{inter} values in molecular systems. In fact, it is considered by several researchers that the contribution from the intramolecular modes in molecular systems is decisive in the pairing process in the superconductivity in doped C_{60}.[22,30] For example, it was reported that the l_{intra} values are much larger than the l_{inter} values in K_3C_{60} and Rb_3C_{60} ($l_{\mathrm{intra}} \geq 10l_{\mathrm{inter}}$).[30] Furthermore, it has also been shown from a neutron-scattering investigation[31] that the electron-libration intermolecular-mode coupling is small in alkali-metal-doped C_{60}. Therefore, we consider only intramolecular electron−phonon coupling in this study. The l_{total} value for the monocations of molecules can be defined as

$$l_{\mathrm{total}} \simeq l_{\mathrm{intra}} = l_{\mathrm{HOMO}} \quad (13)$$

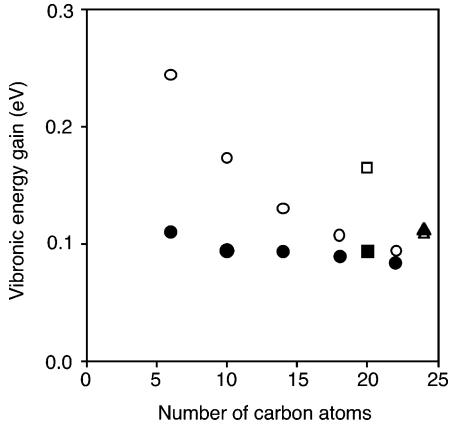

Figure 2. Vibronic energy gain as a function of the number of carbon atoms in acenes, coronene, and corannulene. The opened circles, triangle, and square represent the l_{HOMO} values for acenes, coronene, and corannulene, respectively, and the closed circles, triangle, and square represent the ΔG^0_{HOMO} values for acenes, coronene, and corannulene, respectively.

The l_{HOMO} value for corannulene is defined as

$$l_{HOMO} = \sum_{m=1}^{27} l_{HOMO}(\omega_m) = \sum_{m=1}^{18} g^2_{HOMO}(\omega_m)\hbar\omega_m + \frac{1}{2}\sum_{m=19}^{27} g^2_{HOMO}(\omega_m)\hbar\omega_m \quad (14)$$

The l_{HOMO} values as a function of the number of carbon atoms, N, are shown in Figure 2. The l_{HOMO} value for corannulene is estimated to be 0.165 eV. The l_{HOMO} values were estimated to be 0.244, 0.173, 0.130, 0.107, and 0.094 eV for **1a**, **2a**, **3a**, **4a**, and **5a**, respectively.[23] Therefore, the l_{HOMO} value for corannulene is much larger than those for acenes with similar numbers of carbon atoms. This can be understood as follows. The HOMO of acenes is rather localized on the edge part of carbon atoms, and the HOMO of acenes has nonbonding characteristics. Thus, the orbital interactions between two neighboring carbon atoms are not strong. However, the HOMO of corannulene is somewhat delocalized, and the orbital interactions between two neighboring carbon atoms are strong. Furthermore, acenes have planar structures with D_{2h} geometry, and thus the weak π-orbital interactions are important in the HOMO in acenes. However, corannulene has a bowl-shaped C_{5v} geometry, and thus orbital interactions in the HOMO of corannulene have intermediate characteristics between strong σ-orbital interactions and weak π-orbital interactions. Therefore, the delocalized electronic structures and the intermediate characteristics between the strong σ-orbital interactions and weak π-orbital interactions originating from bowl-shaped C_{5v} geometry are the main reason that the l_{HOMO} value for corannulene is much larger than those for planar D_{2h} symmetric π-conjugated acenes with similar numbers of carbon atoms. The l_{HOMO} values versus the energy level of the HOMO ($-\epsilon_{HOMO}$) are also shown in Figure 3. The ϵ_{HOMO} values are -0.246, -0.213, -0.192, -0.178, -0.169, -0.200, and -0.218 Hartree for **1a**, **2a**, **3a**, **4a**, **5a**, coronene, and corannulene, respectively. Therefore, the stronger bonding HOMO has the greater strength of the electron−phonon interactions.

Possible Electron Pairing in the Monocation of Corannulene

Once the attractive interaction between two electrons dominates over the repulsive screened Coulomb interaction as

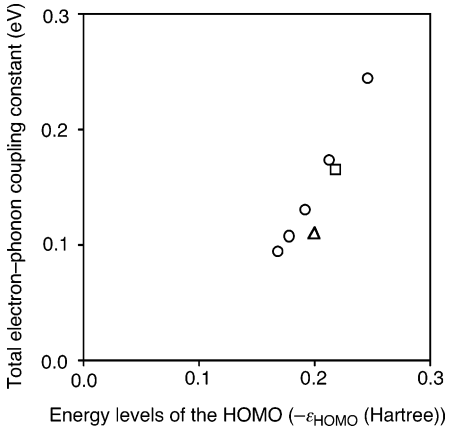

Figure 3. Total electron−phonon coupling constant l_{HOMO} values versus the energy level of the HOMO.

TABLE 2: Necessary Minimum $n(0)$ Values as a Function of μ^* that Satisfy Equation 15 ($-\lambda + \mu^* < 0$)

	$\mu^* =$ 0.10	$\mu^* =$ 0.15	$\mu^* =$ 0.20	$\mu^* =$ 0.25	$\mu^* =$ 0.30
corannulene$^+$	0.606	0.909	1.212	1.515	1.818
coronene$^+$	0.909	1.364	1.818	2.273	2.727
naphthalene$^+$ (**2a**$^+$)	0.578	0.867	1.156	1.445	1.734
anthracene$^+$ (**3a**$^+$)	0.769	1.154	1.538	1.923	2.308
tetracene$^+$ (**4a**$^+$)	0.935	1.402	1.869	2.336	2.804
pentacene$^+$ (**5a**$^+$)	1.064	1.596	2.128	2.660	3.191

expressed by eq 15, the system would produce as many Cooper pairs as possible to lower its energy.

$$-\lambda + \mu^* = -n(0)l_{HOMO} + \mu^* < 0 \quad (15)$$

where μ^* is the dimensionless Coulomb pseudopotential describing the electron−electron repulsion, usually used as a fitting parameter, and ranges between about 0.10 and 0.20 in conventional superconductivity, and $n(0)$ is the density of states at the Fermi level. The $n(0)$ values as a function of μ^* under which $\lambda = \mu^*$ is satisfied are listed in Table 2. For example, considering large l_{HOMO} values estimated above and the usual μ^* values ($\sim$0.20), eq 15 is satisfied if $n(0) > 1.212$ for corannulene. However, considering the l_{HOMO} values for **5a** and the usual μ^* values ($\sim$0.20), eq 15 is satisfied if $n(0) > 2.128$ for **5a**$^+$. We have considered that the $n(0)$ value for the twofold degenerate electronic state in the monocation of benzene is approximately 4, and thus those for the nondegenerate electronic states in the monocations of acenes are approximately 2.[23] However, the $n(0)$ values are obviously sensitive to the overlap (the transfer integral) between the HOMOs on neighboring molecules, and consequently to the distance and the orientation between the molecules and to the extent and the position of the nodes of the HOMO. Therefore, the $n(0)$ values are changeable compared to the physical values, which are related to the intramolecular characteristics such as the l_{HOMO} and $\omega_{ln,HOMO}$ values. Actually, there is the very interesting dependence[32] of T_c upon cell parameter in a variety of systems containing mixtures of alkali metal atoms as fullerene dopants. The overlap integral between adjacent molecules decreases with an increase in the distance between the two adjacent monocations. The $n(0)$ values must increase with a decrease in overlap integral because the total integrated density of states is constant. Assuming that the $\omega_{ln,HOMO}$ and l_{HOMO} values remain invariant to molecular crystal structure differences, the T_c varies simply with $n(0)$. Because the bandwidth decreases with an increase in the distance between corannulene units, there will be some limiting separation where

the delocalized model becomes inappropriate and the electrons localize at large distance between two neighboring molecules. Such an electronic instability will destroy normal metallic behavior as well as superconductivity. In more general terms, superconductivity, usually associated with high $n(0)$ values, often competes with other electronically driven processes in solids. The possibility of electron localization in corannulene as the interunit separation becomes large would be noted, but such high $n(0)$ values often also signal geometrical distortions of the CDW type and ferromagnetic behavior. It was reported that the corannulene cation polymerizes in solution.[33] In this case, the orbital interactions between two neighboring corannulene units are very strong and the $n(0)$ values would be very small even if each unit molecule still has characteristics of electronic structure of each corannulene molecule. Therefore, there is a possibility that the conditions of the attractive electron−electron interactions are not realized under the conditions in which the experimental works in ref 33 were performed. However, as described above, the $n(0)$ values are artificially changeable compared to the physical values, which are related to the intramolecular characteristics such as the l_{HOMO} and $\omega_{ln,HOMO}$ values. The problem is how we can artificially trap the isolated corannulene monocations with an appropriate intermolecular distance in order to realize the conditions of attractive electron−electron interactions. Therefore, if we can artificially increase the distance between two neighboring corannulene monocation units with stable structures so that the $n(0)$ value exceeds about 1.212, then the conditions under which the electron−electron interactions become attractive can be realized.

Intramolecular Electron Mobility in the Monocation of Corannulene

Here, let us consider one-electron transfer assisted by molecular vibrations as a molecular model of the interaction of conduction electrons with vibration.[34,35] From analogy with the definition of the intrinsic intramolecular conductivity, $\sigma_{intra,monocation}$, for the charged hydrocarbons as discussed in previous research,[23] according to the definition suggested by Kivelson and Heeger,[34,35] we define the monocation of corannulene as

$$\sigma_{intra,monocation} \propto \frac{\omega_{HOMO} M_C N}{l_{HOMO}^2} \qquad (16)$$

where M_C denotes the mass of carbon atom, ω_{HOMO} denotes the frequencies of the vibrational modes playing an important role in the electron−phonon interactions, and N denotes the number of carbon atoms. The calculated $\sigma_{intra,monocation}$ values as a function of N are shown in Figure 4. Let us first consider the case that ω_{HOMO} corresponds to the logarithmically averaged phonon frequencies ($\omega_{ln,HOMO}$), which measure the frequencies of the vibronically active modes playing an essential role in the electron−phonon interactions in the monocation of corannulene and have been used widely in order to measure such frequencies. We can see from this figure that the $\sigma_{intra,monocation}$ value increases significantly with an increase in molecular size from **1a** ($\sigma_{intra,monocation} = 14.1 \times 10^5$) to **5a** ($\sigma_{intra,monocation} = 406.0 \times 10^5$). The $\sigma_{intra,monocation}$ value for corannulene ($\sigma_{intra,monocation} = 77.0 \times 10^5$) is much smaller than those for acenes with similar numbers of carbon atoms. In this paper, we introduced the $\omega_{ln,HOMO}$ values, which are usually used in the McMillan's formula[36] described later in order to measure the frequency of the vibrational mode that plays an essential role

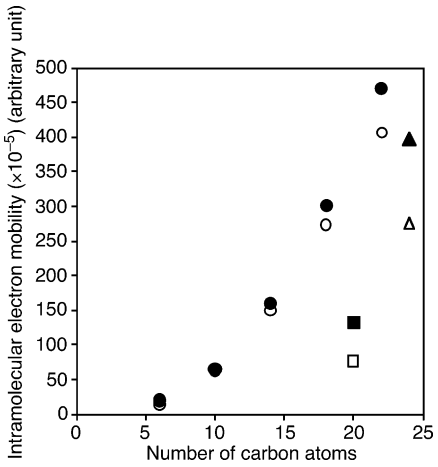

Figure 4. Intramolecular electron mobility as a function of the number of carbon atoms in acenes, coronene, and corannulene. The opened circles, triangle, and square represent these values estimated by considering the $\omega_{ln,HOMO}$ values for acenes, coronene, and corannulene, respectively, and the closed circles, triangle, and square represent these values estimated by considering the frequencies of the vibrational modes that play the most essential role in the electron−phonon interactions for acenes, coronene, and corannulene, respectively.

in the electron−phonon interactions. Of course, other definitions of averaged phonon frequencies as well as the $\omega_{ln,HOMO}$ values are also available if the values approximately indicate the frequency of the vibrational modes that play an essential role in the electron−phonon interactions. In this sense, it should be noted that the $\omega_{ln,HOMO}$ values may not have strict physical meaning but may be the approximate values by which we qualitatively discuss which frequency modes play an essential role in the electron−phonon interactions. Let us next consider the $\sigma_{intra,monocation}$ values estimated by considering the case that the ω_{HOMO} values correspond to the frequencies of the vibrational modes that play the most important role in the electron−phonon interactions (i.e., 1656, 1630, 1610, 1594, 1572, 1668, and 1498 cm^{-1} for **1a**, **2a**, **3a**, **4a**, **5a**, coronene, and corannulene, respectively). Even though the $\sigma_{intra,monocation}$ values estimated by considering the frequency of only the vibrational modes playing the most important role in the electron−phonon interactions are somewhat larger than those estimated by considering the $\omega_{ln,HOMO}$ values, in particular, in **5a**, coronene, and corannulene, essential qualitative results obtained by considering the frequency of only the vibrational modes playing the most important role in the electron−phonon interactions are similar to those obtained by considering the $\omega_{ln,HOMO}$ values. Therefore, the $\omega_{intra,monocation}$ values are much more sensitive to the strengths of the electron−phonon interactions than to the frequencies of vibrational modes in the molecules under consideration. As described in the previous section, the l_{HOMO} value for corannulene is larger than those for acenes with similar numbers of carbon atoms. Therefore, the larger l_{HOMO} value for corannulene than those for acenes, due to the electronic structure difference between them originating from the structural difference between corannulene with the bowl-shaped C_{5v} symmetry and π-conjugated acenes with the planar D_{2h} symmetry, is the main reason that the $\sigma_{intra,monocation}$ value for corannulene is much smaller than those for acenes with similar numbers of carbon atoms.

Intermolecular Electron Transfer

Reorganization Energy. Let us next discuss the electron transfer through the corannulene molecule, which is of interest

TABLE 3: Ionization Energy, Electron Affinity, Hopping Barrier, and Reorganization Energy (eV) in the Positively Charged Corannulene

$(C_{20}H_{10}^{+})(C_{20}H_{10}) \rightarrow (C_{20}H_{10})(C_{20}H_{10}^{+})$	
ionization energy	0.116
electron affinity	−0.125
hopping barrier	0.241
reorganization energy	0.060

for possible nanoelectronics applications. Here, we will estimate the reorganization energy for elementary charge transfer. We optimized the structures of the monocation of corannulene. The estimated ionization energy, electron affinity, hopping barrier, and reorganization energy between the neutral molecule and the monocation are listed in Table 3.

Denoting the adiabatic ionization energy as I_0, the vertical (fixed geometry) ionization from the ground state of neutral corannulene costs an energy of $I_0 + 0.116$ eV, whereas the electron affinity of the monocation of corannulene (at its optimum geometry) is $I_0 - 0.125$ eV. Thus, the isolated neutral corannulene and the monocation of the corannulene molecule with their optimum structures lead to a hopping barrier of 0.241 eV (ignoring polarization of the environment, which might increase the barrier). Considering the Marcus-type electron transfer diagram, a net barrier can be estimated to be $\sim 0.241/4 = 0.060$ eV. It should be noted that electronic interactions (orbital overlap) and steric interactions are ignored when we estimate the reorganization energies between the neutral molecule and the monocation. For a good conductor with rapid electron transfer, the overlap of the HOMOs of these molecules should be sufficiently large. This requires an interaction energy greater than the barrier of 0.060 eV for corannulene.

Optimized Structures of the Monocation of Corannulene. Let us next look into the optimized structures of the monocation of corannulene. To compare the calculated results for the monocation to that for the neutral molecule, the optimized C−C bond lengths of the neutral molecule and the monocation in corannulene are listed in Table 4. Let us first look into the C−C bond lengths of the hub moiety. The d_1 and d_3 values become larger (smaller) by hole doping in corannulene$^{+}_{A}$ (corannulene$^{+}_{B}$), and the d_2 value becomes smaller (larger) by hole doping in corannulene$^{+}_{A}$ (corannulene$^{+}_{B}$). That is, the C−C bond lengths in the hub moiety that are lengthened (shortened) by hole doping in corannulene$^{+}_{A}$ are shortened (lengthened) by hole doping in corannulene$^{+}_{B}$. This can be understood as follows. The atomic orbitals between two neighboring carbon atoms that are combined in phase (out of phase) in the HOMO (A) are combined out of phase (in phase) in the HOMO (B) in the hub moiety of corannulene. The C−C bonds formed by two neighboring carbon atoms that are combined in phase (out of phase) in the HOMO become longer (shorter) when an electron is removed from the HOMO. This is the reason that the C−C bond lengths in the hub moiety that are lengthened (shortened) by hole doping in corannulene$^{+}_{A}$ are shortened (lengthened) by hole doping in corannulene$^{+}_{B}$. It should be noted that the C−C bond lengths in the hub moiety change much more significantly by hole doping than those in other moieties. This can be understood as follows. The electron density on the carbon atoms in the hub moiety in the HOMO is much higher than that on other carbon atoms. Therefore, the orbital interactions between two neighboring carbon atoms in the hub moiety are much stronger than those in another moieties. This is the reason that the C−C bond lengths in the hub moiety change much more significantly by hole doping than those in another moieties. Let us next look into the spoke moiety. The d_4, d_5, and d_6 values become larger by hole doping in both corannulene$^{+}_{A}$ and corannulene$^{+}_{B}$. This is because the atomic orbitals between two neighboring carbon atoms that form the spoke moiety are combined in phase in both HOMO (A) and HOMO (B). Let us next look into the rim moiety. Apart from the d_9 values in corannulene$^{+}_{B}$, the C−C bond lengths become larger by hole doping in the rim moiety in both corannulene$^{+}_{A}$ and corannulene$^{+}_{B}$. This is because the atomic orbitals between two neighboring carbon atoms forming a rim in the HOMO are combined in phase, and those between two neighboring carbon atoms whose bond length is d_9 are combined out of phase in the HOMO (B). Let us next look into the flank moiety. The C−C bonds formed by two neighboring carbon atoms that are combined in phase (out of phase) in the flank moiety in the HOMO become longer (shorter) by hole doping in both corannulene$^{+}_{A}$ and corannulene$^{+}_{B}$. Let us next look into the relationships between the optimized structures of the monocations and the electron−phonon coupling constants. We can see from Figure 1 and Table 4 that the E_2 mode of 1498 cm^{-1} is the main mode converting the D_{6h} symmetric neutral structure to the D_{2h} symmetric structures of the monocations. We can also confirm the calculated results from the fact that the E_2 mode of 1498 cm^{-1} plays the most essential role in the electron−phonon interactions in the monocation of corannulene. However, it should be noted that this calculated result does not mean that only one E_2 mode of 1498 cm^{-1} carries all of the coupling strength and determines the optimized structures of the monocations. In fact, the E_2 modes of 439, 648 cm^{-1}, and so on, as well as the E_2 mode of 1498 cm^{-1}, play a role in the electron−phonon interactions.

The relative bowl depth defined by the distance from the best plane of the five carbon atoms of the central hubs to the best plane of the 10 carbon atoms in the rims is 0.86 Å in neutral corannulene, and that is 0.84 Å in the monocation of corannulene. Therefore, the relative bowl depth decreases by only 0.02 Å by hole doping in corannulene.

TABLE 4: Optimized C−C Bond Lengths of the Neutral Molecule and the Monocation of Corannulene[a]

	d_1	d_2	d_3	d_4	d_5	d_6	d_7
corannulene	1.417	1.417	1.417	1.385	1.385	1.385	1.390
corannulene$^{+}_{A}$	1.428 (+0.011)	1.392 (−0.088)	1.446 (+0.029)	1.394 (+0.009)	1.388 (+0.003)	1.396 (+0.011)	1.404 (+0.014)
corannulene$^{+}_{B}$	1.409 (−0.008)	1.440 (+0.023)	1.386 (−0.031)	1.387 (+0.002)	1.395 (+0.010)	1.394 (+0.009)	1.395 (+0.005)

d_8	d_9	d_{10}	d_{11}	d_{12}	d_{13}	d_{14}
1.390	1.390	1.448	1.448	1.448	1.448	1.448
1.390 (±0.000)	1.421 (+0.031)	1.440 (−0.008)	1.439 (−0.009)	1.449 (+0.001)	1.447 (−0.001)	1.430 (−0.018)
1.416 (+0.026)	1.389 (−0.001)	1.446 (−0.002)	1.444 (−0.004)	1.434 (−0.014)	1.431 (−0.017)	1.450 (+0.002)

[a] The values in parentheses indicate the changes of the C−C bond lengths by hole doping. The labels A and B in corannulene$^{+}_{A}$ and corannulene$^{+}_{B}$ represent the optimized structures of the monocations in which the HOMO (A) and HOMO (B) shown in Figure 1 are partially occupied by an electron, respectively

TABLE 5: Average Changes of the C−C Bond Lengths by Hole Doping in Coronene and Corannulene

	hub	spoke	rim	flank	whole
coronene	0.007	0.007	0.011	0.010	0.009
corannulene	0.032	0.018	0.012	0.004	0.014

Comparison of the Calculated Results of Corannulene to Those of Coronene

Let us next compare the calculated results for the monocation of corannulene to those for the monocation of coronene.[23] The graphite intercalation compounds (GICs) exhibit superconductivity,[37] but in contrast to the A_3C_{60} complexes the T_c values of the GICs are low, the highest transition temperature being 5.5 K in C_4K.[38,39] The reader can refer to useful discussions on the superconductivity of the GICs in a review paper.[40] It is important to consider why the A_3C_{60} complexes show high T_c values. The remarkable contrast between the high-T_c superconductivity of the A_3C_{60} complexes and the low-T_c superconductivity of the GICs can be derived from the fact that the C_{60} molecule involves a bowl-shaped structure but the graphite sheet is planar. The discussion of Haddon[41] on the rehybridization of the π-orbitals and the 2s atomic orbital may be useful for the understanding of the high-T_c superconductivity of the A_3C_{60} complexes. It is quite interesting to characterize the electronic features of corannulene and coronene in that corannulene and coronene can be viewed as fragments of C_{60} and graphite, respectively. In this section, we discuss how the structural difference between corannulene and coronene affects the vibronic interactions in these hydrocarbon cations.

The E_{2g} modes of 370 and 1668 cm^{-1} afford large electron−phonon coupling constants in the monocation of coronene. As in the monocation of corannulene, the electron−phonon coupling constants for the twofold degenerate E_{2g} modes are much larger than those for the nondegenerate A_{1g} modes in the monocation of coronene. The l_{HOMO} value for planar D_{6h} symmetric π-conjugated coronene (0.110 eV) is smaller than that for corannulene (0.165 eV) even though the number of carbon atoms of coronene is not significantly different from that of corannulene. The $\omega_{ln,HOMO}$ value for coronene was estimated to be 1162 cm^{-1}.[23] Therefore, the $\omega_{ln,HOMO}$ value for corannulene is smaller than that for coronene. As described in the previous section, the intermediate characteristics between strong σ-orbital interactions and weak π-orbital interactions in the HOMO of corannulene are the main reason for the calculated results.

Let us next compare the optimized structures of the monocation of corannulene to those of the monocation of coronene. To compare the calculated results for the monocation of corannulene to those for the monocation of coronene, the average changes of the C−C bond lengths by hole doping defined by eq 17 in the hub, spoke, rim, and flank moieties in corannulene and coronene are listed in Table 5.

$$\Delta d_{av} = \frac{1}{n_{total}} \sum_{i}^{n_{total}} |d_i(\text{neutral}) - d_i(\text{monocation})| \quad (17)$$

where d_i(neutral) and d_i(monocation) denote the distances between two neighboring carbon atoms in the neutral molecule and monocation, respectively, and n_{total} denotes the total number of C−C bonds.

We can see from Table 5 that the C−C bond lengths in the hub moiety change much more significantly by hole doping in corannulene than in coronene. This can be understood in view of the phase patterns of the HOMO in coronene and corannulene. In the HOMO of coronene, the electron density on carbon atoms forming an inner ring is lower than that on carbon atoms forming an outer ring. Therefore, the orbital interactions between two neighboring carbon atoms in the hub moiety in the HOMO of coronene are not strong. However, in the HOMO of corannulene, the electron density on carbon atoms forming an inner ring is higher than that on carbon atoms forming an outer ring. Therefore, the orbital interactions between two neighboring carbon atoms in the hub moiety in the HOMO of corannulene are strong. This is the reason that the C−C bond lengths in the hub moiety change more significantly by hole doping in corannulene than in coronene. In a similar way, the change of the C−C bond lengths in another moiety is also rationalized in view of the phase patterns of the HOMO. Let us next look into the C−C bond lengths of the whole molecule. We can see from Table 5 that the C−C bonds change more significantly by hole doping in corannulene than in coronene. The strong orbital interactions between two neighboring carbon atoms originating from the intermediate characteristics between strong σ-orbital interactions and weak π-orbital interactions are the main reason that the C−C bond lengths in bowl-shaped corannulene change more significantly by hole doping than those in planar coronene.

The $\sigma_{intra,monocation}$ value for coronene ($\sigma_{intra,monocation} = 276.6 \times 10^5$) is much larger than that for corannulene ($\sigma_{intra,monocation} = 77.0 \times 10^5$). The reorganization energy between the neutral molecule and its monocation in coronene was estimated to be 0.028 eV. Therefore, the reorganization energy for the positively charged corannulene is larger than that for the positively charged coronene. The larger $n(0)$ values are needed for the positively charged corannulene to become a good conductor compared to those for the positively charged coronene. This is because the orbital interactions between two neighboring carbon atoms in the HOMO in corannulene are stronger than those in coronene, and thus the l_{HOMO} value for corannulene is larger than that for coronene.

Relationships between Normal and Superconducting States

Let us next look into the relationships between the electron transfer and the electron−phonon interactions in the positively charged bowl-shaped corannulene and planar acenes and coronene. Intramolecular electron mobility, intermolecular charge transfer, and attractive electron−electron interactions are shown schematically in Figure 5. In Figure 6, the reorganization energies as a function of the total electron−phonon coupling constants are shown. In view of Figure 6, a plot of the reorganization energies against the total electron−phonon coupling constants is found to be nearly linear. The reorganization energies between the neutral molecule and the corresponding monocation for **3a**, **4a**, and **5a** were estimated to be 0.034, 0.027, and 0.022 eV, respectively.[23] Therefore, the reorganization energy between the neutral molecule and the corresponding monocation for corannulene is larger than those for coronene and acenes with similar numbers of carbon atoms.

As discussed in the previous section, the $\sigma_{intra,monocation}$ values are inversely proportional to the l^2_{HOMO} values and are proportional to the ω_{HOMO} values. Therefore, the $\sigma_{intra,monocation}$ values for π-conjugated coronene and acenes are larger than that for corannulene. This is because the l_{HOMO} values for corannulene are larger than those for π-conjugated coronene and acenes.

The reorganization energy between the neutral molecule and the corresponding monocation for corannulene is larger than those for coronene and acenes with similar numbers of carbon atoms. This means that in order for the positively charged corannulene to become a good conductor the larger overlap integral is needed (the $n(0)$ values should not be too large)

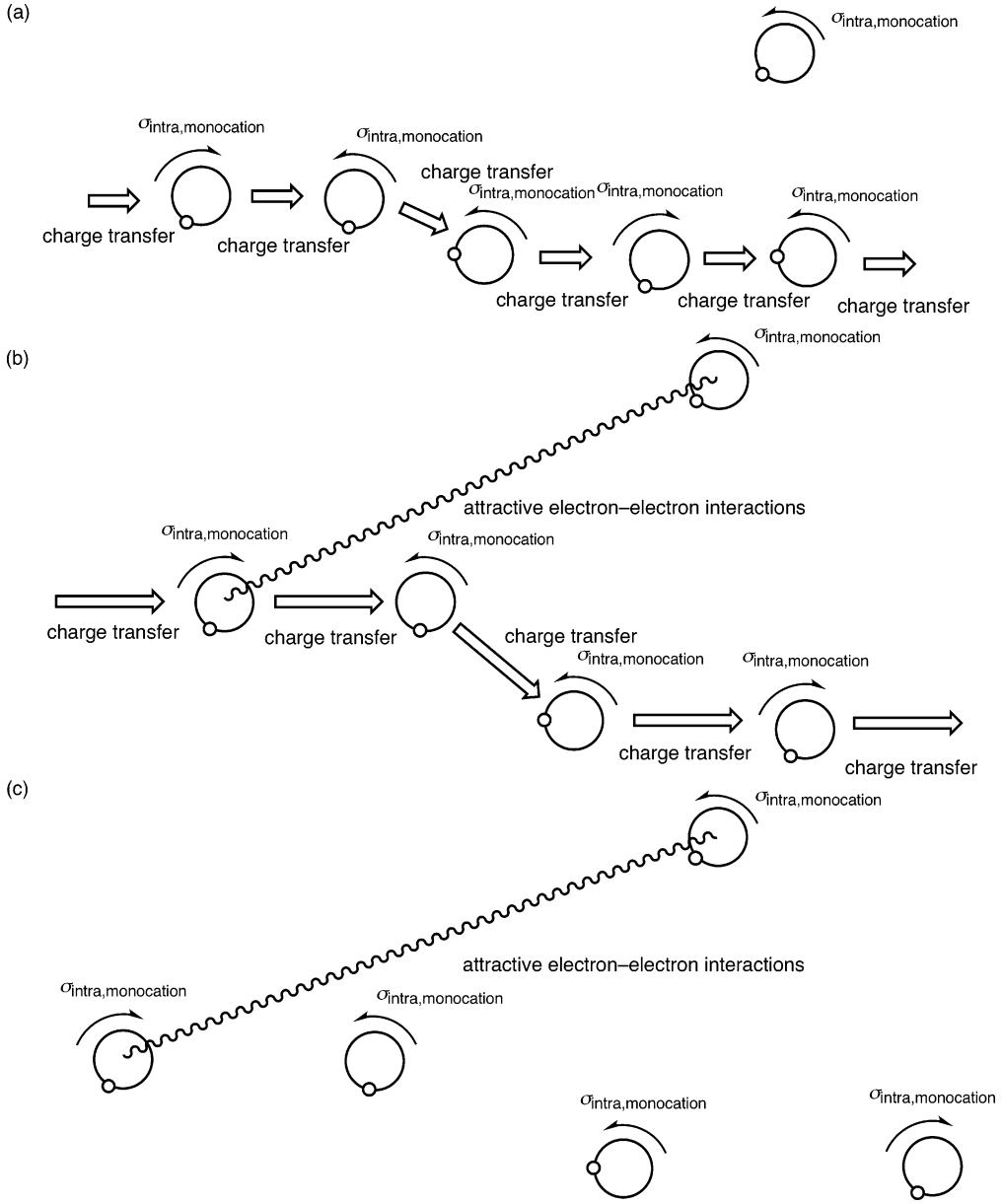

Figure 5. Intramolecular electron mobility, intermolecular charge transfer, and attractive electron−electron interactions in the monocations of hydrocarbons. (a) The condition under which normal metallic states are realized, but the condition under which the attractive electron−electron interactions are not realized ($n(0)$ value is too small for the attractive electron−electron interactions to be realized). (b) The condition under which normal metallic state and attractive electron−electron interactions are realized ($n(0)$ value is appropriate for both metallic state and the attractive electron−electron interactions to be realized). (c) The condition under which normal metallic states are not realized, but the condition under which the attractive electron−electron interactions are realized ($n(0)$ value is too large for the normal metallic state to be realized). The larger the l_{HOMO} values are, the smaller the appropriate $n(0)$ values satisfying the condition b are.

compared to those for the positively charged coronene and acenes (Figure 5). This may be because the orbital interactions between two neighboring carbon atoms in the HOMO of corannulene are stronger than those for coronene and acenes with similar numbers of carbon atoms. This is also closely related to the calculated result that the l_{HOMO} value for corannulene is larger than those of coronene and acenes with similar numbers of carbon atoms.

The conditions under which eq 15 is satisfied are more difficult to be realized in the monocations of coronene and acenes with similar numbers of carbon atoms than in the monocation of corannulene because the l_{HOMO} values for coronene and acenes are smaller than that for corannulene. We can see from eq 15 that large $n(0)$ and l_{HOMO} values are favorable for the realization of the condition under which the electron−electron interactions become attractive (Figure 5c and c). However, when the $n(0)$ values are too large (the orbital overlap is too small), the molecular crystal does not become metallic, as discussed above. Furthermore, considering that the l_{HOMO} values are proportional to the reorganization energies, and the $\sigma_{intra,monocation}$ values are inversely proportional to l_{HOMO}^2, a large l_{HOMO} value would not be favorable for normal metallic behavior.

We can evaluate possible T_c values for the monocations of hydrocarbons by using the approximate solution of the Eliashberg equation[42] from the electron−phonon coupling constants. We can estimate T_c values using McMillan's formula[36] defined as

$$T_c = \frac{\omega_{ln,HOMO}}{1.2} \exp\left[-\frac{1.04\{1 + n(0)l_{HOMO}\}}{n(0)l_{HOMO} - \mu^*\{1 + 0.62n(0)l_{HOMO}\}}\right] \quad (18)$$

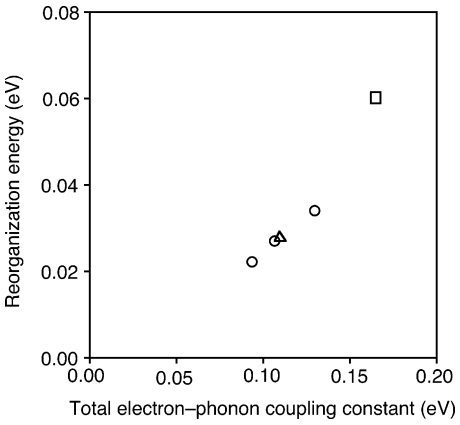

Figure 6. Reorganization energies as a function of the total electron−phonon coupling constants in the positively charged acenes, coronene, and corannulene. The circles, triangle, and square represent these values for acenes, coronene, and corannulene, respectively.

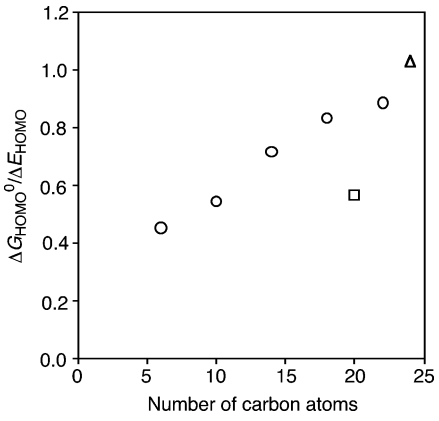

Figure 7. Ratio of the lowest order quantum corrections (ΔG^0_{HOMO}) to the classical potential-lowering energy term (ΔE_{HOMO}). The circles, triangle, and square represent these values for acenes, coronene, and corannulene, respectively.

It should be noted that McMillan's formula was derived from a three-dimensional formalism, while the electron (hole) carriers in the monocations under consideration would not form a three-dimensional system. However, we believe that McMillan's formula is valid at least for qualitative discussion in this research. The T_c values for the monocation of corannulene would be larger than those for the monocations of coronene and acenes with similar numbers of carbon atoms because the l_{HOMO} value for corannulene is larger than those for coronene and acenes with similar numbers of carbon atoms. Although, at the same time, large l_{HOMO} values are not favorable for a molecular crystal to become metallic as mentioned above. In summary, in order for the monocation of corannulene to become a good conductor, larger orbital overlaps (smaller $n(0)$ values) are needed compared to the case of the monocations of coronene and acene with similar numbers of carbon atoms, and the smaller $n(0)$ values are enough for the conditions under which the electron−electron interactions become attractive to be realized in the monocation of corannulene than in the monocations of coronene and acenes with similar numbers of carbon atoms. And once the condition under which they can become metallic is realized, and furthermore, the conditions of attractive electron−electron interactions and the occurrence of superconducting states are realized, the monocation of corannulene would become a higher temperature superconductor than the monocations of coronene and acenes with similar numbers of carbon atoms.

Multimode Problem

To investigate how the consideration of the multimode problem is closely related to the characteristics of the electron−phonon interactions, let us next handle the difficult multimode problem, which we ignore in the previous sections in this paper. It is important for us to treat the multimode problem because the vibronic coupling redetermines the vibrational frequencies. According to ref 43, the relevant ground-state energetics for the multimode problems in the case of $e\otimes(nE)$ are defined as

$$\Delta E_{HOMO} = l_{HOMO} + \Delta G^0_{HOMO} \quad (19)$$

The ΔG^0_{HOMO} represents the lowest order quantum corrections that originate from the change of the frequencies of the vibronic modes as a consequence of the vibronic coupling. For example, the relevant ground-state energetics for the multimode problems in case of $e\otimes(nE)$ are defined as

$$\Delta E_{HOMO} = \sum_m \hbar\omega_m g^2_{HOMO}(\omega_m) + \frac{1}{2}\sum_m \hbar(\omega_m - \nu_m) \quad (20)$$

where ν_m is the new frequency that is redetermined as a consequence of the vibronic coupling and is the solution (ν) of the equation

$$\left(\sum_m \omega_m g^2_{HOMO}(\omega_m)\right)^{-1} \sum_m \frac{g^2_{HOMO}(\omega_m)\omega_m{}^3}{\omega_m{}^2 - \nu^2} = 1 \quad (21)$$

This method is based on the approximate calculation of the new vibrational normal-mode frequencies, ν_m, arising after vibronic coupling. Of these modes, $n - 1$ falls in the interval between the successive original bare mode frequencies; the remaining one is a zero mode $\nu_1 = 0$. The ν_m values for E_2 vibrational modes in corannulene are listed in Table 6. The relevant ground-state energetics, ΔE_{HOMO}, for the multimode problems by using eq 20 in the monocations under consideration are listed in Table 7. Furthermore, the ΔG^0_{HOMO} values as well as the l_{HOMO} values are shown in Figure 2. The ratio of the lowest order quantum corrections (ΔG^0_{HOMO}) to the classical potential-lowering energy term (ΔE_{HOMO}) are shown in Figure 7. The ΔG^0_{HOMO} values are estimated to be 0.093 and 0.113 eV for corannulene and coronene, respectively. Furthermore, the ΔG^0_{HOMO} values are estimated to be 0.110, 0.094, 0.093, 0.089, and 0.083 eV for **1a**, **2a**, **3a**, **4a**, and **5a**, respectively. Therefore, compared to the l_{HOMO} values, the ΔG^0_{HOMO} values do not change significantly with an increase in molecular size. The ΔE_{HOMO} values are estimated to be 0.259 and 0.222 eV for corannulene and coronene, respectively. Furthermore, the ΔE_{HOMO} values are estimated to be 0.354, 0.268, 0.223, 0.197, and 0.177 eV for **1a**, **2a**, **3a**, **4a**, and **5a**, respectively. Therefore, fundamental aspects of the relationships between the ΔE_{HOMO} values and the molecular sizes and structures are similar to those between the l_{HOMO} values and the molecular sizes and structures. This is because the ΔG^0_{HOMO} values do not change significantly with an increase in molecular size. The $\Delta G^0_{HOMO}/l_{HOMO}$ values are estimated to be 0.564 and 1.027 for corannulene and coronene, respectively. And the $\Delta G^0_{HOMO}/l_{HOMO}$ values are estimated to be 0.451, 0.543, 0.715, 0.832, and 0.883 for **1a**, **2a**, **3a**, **4a**, and **5a**, respectively. Therefore, apart from bowl-shaped corannulene, the $\Delta G^0_{HOMO}/l_{HOMO}$ values increase with

TABLE 6: New Vibrational Normal-Mode Frequencies ν_m Arising after Vibronic Coupling of the Monocation of Corannulene in Case of $e\otimes(nE)$

ω_m (cm^{-1})	E_2 (142)	E_2 (282)	E_2 (439)	E_2 (548)	E_2 (613)	E_2 (648)	E_2 (773)	E_2 (813)	E_2 (970)
$g_{HOMO}(\omega_m)$	0.640	0.359	0.720	0.069	0.169	0.463	0.205	0.150	0.017
$\omega_m g^2_{HOMO}(\omega_m)$ (cm^{-1})	58.16	36.34	227.58	2.61	17.51	138.91	32.49	18.29	0.28
ν_m (cm^{-1})	0	196	307	545	566	618	755	805	969
$\omega_m - \nu_m$ (cm^{-1})	142	86	132	3	47	30	18	8	1

E_2 (1092)	E_2 (1172)	E_2 (1197)	E_2 (1392)	E_2 (1441)	E_2 (1498)	E_2 (1669)	E_2 (3176)	E_2 (3192)	total
0.269	0.105	0.068	0.157	0.070	0.537	0.056	0.004	0.003	
79.02	12.92	5.53	34.31	7.06	431.98	5.23	0.05	0.03	1108.3
922	1159	1192	1250	1402	1442	1667	3176	3192	
170	13	5	142	39	56	2	0	0	894

TABLE 7: Relevant Ground-State Energetics (in meV) for Multimode Problems in the Monocations

	corannulene	coronene	**1a**	**2a**	**3a**	**4a**	**5a**
ΔE_{HOMO} (eq 20)	258.7	222.5	354.4	267.6	223.2	196.7	176.7
ΔE_{HOMO} (eq 22)	252.7	221.3	354.1	267.6	223.2	196.9	176.5

an increase in molecular size in planar molecules such as acenes and coronene. In general, the high and low-frequency modes, play less- and more-, respectively, important roles in the electron−phonon interactions with an increase in molecular size, and thus the multimode problem would be more important with an increase in molecular size.

Let us next look into O'Brien's effective-mode approximation.[44] According to ref 44, we estimate the ΔG^0_{HOMO} values as well as the l_{HOMO} values, defined in eq 22, for example, in case of $e\otimes(nE)$

$$\Delta E_{HOMO} = \sum_m \hbar\omega_m g^2_{HOMO}(\omega_m) + \frac{1}{4}\left\{\frac{\sum_m \hbar\omega_m^2 g^2_{HOMO}(\omega_m)}{\sum_m \omega_m g^2_{HOMO}(\omega_m)} + \frac{\sum_m \hbar\omega_m g^2_{HOMO}(\omega_m)}{\sum_m g^2_{HOMO}(\omega_m)}\right\} \quad (22)$$

The ΔE_{HOMO} values estimated by this equation are listed in Table 7. We can see from this table that the ΔE_{HOMO} values estimated by this equation are in excellent agreement with those estimated by eq 20.

Concluding Remarks

We studied the electron−phonon interactions in the monocation of corannulene. Our calculated results show that the C−C stretching E_2 mode of 1498 cm^{-1} most strongly couples to the e_1 HOMO in corannulene. In addition to this E_2 mode, the low-frequency E_2 modes of 439 and 648 cm^{-1} also strongly couple to the e_1 HOMO in corannulene. The estimated l_{HOMO} value for corannulene is 0.165 eV. The l_{HOMO} value for corannulene is much larger than those for acenes with similar numbers of carbon atoms. The HOMO of acenes is rather localized on the edge part of the carbon atoms, and the HOMO of acenes has nonbonding characteristics. Thus, the orbital interactions between two neighboring carbon atoms are not strong. However, the HOMO of corannulene is somewhat delocalized, and the orbital interactions between two neighboring carbon atoms are strong. Furthermore, acenes have planar structures with D_{2h} geometry, and thus the weak π-orbital interactions are important in the HOMO in acenes. However, corannulene has a bowl-shaped C_{5v} geometry, and thus orbital interactions in the HOMO of corannulene have intermediate characteristics between strong σ-orbital interactions and weak π-orbital interactions. Therefore, the delocalized electronic structures and the intermediate characteristics between the strong σ-orbital interactions and weak π-orbital interactions originating from bowl-shaped C_{5v} geometry are the main reason that the l_{HOMO} value for corannulene is much larger than those for planar coronene and acenes with similar numbers of carbon atoms. Although only the C−C stretching modes around 1500 cm^{-1} play an essential role in the electron−phonon interactions in the monocations of acenes, the low-frequency modes as well as the C−C stretching modes play an important role in the electron−phonon interactions in the monocation of corannulene.

We also discussed the intramolecular electron mobility in the monocation of corannulene. The $\sigma_{intra,monocation}$ value for corannulene is estimated to be much smaller than those for coronene and acenes with similar numbers of carbon atoms. The larger l_{HOMO} value for corannulene than those for coronene and acenes, due to the electronic structure difference between them originating from the structural difference between corannulene with the bowl-shaped C_{5v} symmetry and coronene and acenes with planar structures, is the main reason for the calculated results. We optimized the structures of the monocation of corannulene and also discussed the single charge transfer through the corannulene molecule. The reorganization energy between the neutral molecule and the monocation in corannulene is estimated to be 0.060 eV. The reorganization energy for the positively charged corannulene is larger than those for the positively charged acenes with similar numbers of carbon atoms. In order for the monocation of corannulene to become a good conductor, larger orbital overlaps (smaller $n(0)$ values) are needed compared to the case of the monocations of coronene and acene with similar numbers of carbon atoms, and the smaller $n(0)$ values are enough for the conditions under which the electron−electron interactions become attractive to be realized in the monocation of corannulene than in the monocations of coronene and acenes with similar numbers of carbon atoms. And once the condition under which they can become metallic is realized, and furthermore, the conditions of attractive electron−electron interactions and the occurrence of superconducting states are realized, the monocation of corannulene would become a higher temperature superconductor than the monocations of coronene and acenes with similar numbers of carbon atoms.

We also treated multimode problem in order to investigate how consideration of the multimode problem is closely related to the characteristics of the electron−phonon interactions. Compared to the l_{HOMO} values, the ΔG^0_{HOMO} values do not change significantly with an increase in molecular size. Therefore, fundamental aspects of the relationships between the

ΔE_{HOMO} values and the molecular sizes and structures are similar to those between the l_{HOMO} values and the molecular sizes and structures. The $\Delta G^0_{HOMO}/l_{HOMO}$ values increase with an increase in molecular size in planar molecules such as acenes and coronene. This means that the ΔG^0_{HOMO} terms become more important with an increase in molecular size.

Acknowledgment. This study was performed under the Project of Academic Frontier Center at Nagasaki Institute of Applied Science. This work is partly supported by a Grant-in-Aid for Scientific Research from the Japan Society for the Promotion of Science (JSPS-16560618, JSPS-17350094).

References and Notes

(1) (a) Bersuker, I. B. *The Jahn−Teller Effect and Vibronic Interactions in Modern Chemistry*; Plenum: New York, 1984. (b) Bersuker, I. B.; Polinger, V. Z. *Vibronic Interactions in Molecules and Crystals*; Springer: Berlin, 1989. (c) Bersuker, I. B. *Chem. Rev.* **2001**, *101*, 1067.

(2) Grimvall, G. *The Electron−Phonon Interaction in Metals*; North-Holland: Amsterdam, 1981.

(3) Fischer, G. *Vibronic Coupling: The Interaction between the Electronic and Nuclear Motions*; Academic: London, 1984.

(4) (a) Lipari, N. O.; Duke, C. B.; Pietronero, L. *J. Chem. Phys.* **1976**, *65*, 1165. (b) Pulay, P.; Fogarasi, G.; Boggs, J. E. *J. Chem. Phys.* **1981**, *74*, 3999.

(5) (a) Kittel, C. *Quantum Theory of Solids*; Wiley: New York, 1963. (b) Ziman, J. M. *Principles of the Theory of Solids*; Cambridge University: Cambridge, 1972. (c) Ibach, H.; Lüth, H. *Solid-State Physics*; Springer: Berlin, 1995. (d) Burdett, J. K. *Chemical Bonding in Solids*; Oxford University Press.: Oxford, U.K., 1995. (e) Mizutani, U. *Introduction to the Electron Theory of Metals*; Cambridge University Press.: Cambridge, U.K., 2001.

(6) (a) Schrieffer, J. R. *Theory of Superconductivity*; Addison-Wesley: MA, 1964. (b) de Gennes, P. G. *Superconductivity of Metals and Alloys*; Benjamin: New York, 1966.

(7) Little, W. A. *Phys. Rev.* **1964**, *134*, A1416.

(8) (a) Jérome, D.; Mazaud, A.; Ribault, M.; Bechgaad, K. *J. Phys. Lett.* (France) **1980**, *41*, L95. (b) Ribault, M.; Benedek, G.; Jérome, D.; Bechgaad, K. *J. Phys. Lett.* (France) **1980**, *41*, L397.

(9) Reviews and books: (a) Jérome, D.; Schulz, H. J. *Adv. Phys.* **1982**, *31*, 299. (b) Ishiguro, T.; Yamaji, K. *Organic Superconductors*; Springer: Berlin, 1990. (c) Williams, J. M.; Ferraro, J. R.; Thorn, R. J.; Karlson, K. D.; Geiser, U.; Wang, H. H.; Kini, A. M.; Whangbo, M.-H. *Organic Superconductors*; Prentice Hall: New Jersey, 1992.

(10) (a) Barth, W. E.; Lawton, R. G. *J. Am. Chem. Soc.* **1966**, *88*, 380. (b) Barth, W. E.; Lawton, R. G. *J. Am. Chem. Soc.* **1971**, *93*, 1730.

(11) Gleicher, G. J. *Tetrahedron* **1967**, *23*, 4257.

(12) Hanson, J. C.; Nordman, C. E. *Acta Crystallogr., Sect. B* **1976**, *B32*, 1147.

(13) (a) Scott, L. T.; Hashemi, M. M.; Meyer, D. T.; Warren, H. B. *J. Am. Chem. Soc.* **1991**, *113*, 7082. (b) Scott, L. T.; Hashemi, M. M.; Bratcher, M. S. *J. Am. Chem. Soc.* **1992**, *114*, 1920. (c) Borchardt, A.; Fuchicello, A.; Kilway, K. V.; Baldridge, K. K.; Siegel, J. S. *J. Am. Chem. Soc.* **1992**, *114*, 1921.

(14) Kroto, H. W.; Heath, J. R.; O'Brien, S. C.; Curl, R. F.; Smalley, R. E. *Nature* **1985**, *318*, 162.

(15) Krätschmer, W.; Lamb, L. D.; Fostiropoulos, K.; Huffman, D. R. *Nature* **1990**, *347*, 354.

(16) (a) Ayalon, A.; Rabinovitz, M.; Cheng, P.-C.; Scott, L. T. *Angew. Chem., Int. Ed. Engl.* **1992**, *31*, 1636. (b) Baumgarten, M.; Gherghel, L.; Wagner, M.; Weitz, A.; Rabinovitz, M.; Cheng, P.-C.; Scott, L. T. *J. Am. Chem. Soc.* **1995**, *117*, 6254. (c) Ayalon, A.; Sygula, A.; Cheng, P.-C.; Rabinovitz, M.; Rabideau, P. W.; Scott, L. T. *Science* **1994**, *265*, 1065.

(17) (a) Peck, R. C.; Schulman, J. M.; Disch, R. L. *J. Phys. Chem.* **1990**, *94*, 6637. (b) Abdourazak, A. H.; Sygula, A.; Rabideau, P. W. *J. Am. Chem. Soc.* **1993**, *115*, 3010. (c) Rabideau, P. W.; Marcinow, Z.; Sygula, R.; Sygula, A. *Tetrahedron Lett.* **1993**, *34*, 6351. (d) Disch, R. L.; Schulman, J. M. *J. Am. Chem. Soc.* **1994**, *116*, 1533. (e) Sygula, A.; Rabideau, P. W. *J. Chem. Soc., Chem. Commun.* **1994**, 1497. (f) Martin, J. M. L. *Chem. Phys. Lett.* **1996**, *262*, 97. (g) Tanaka, K.; Sato, T.; Okada, M.; Yamabe, T. *Fullerene Sci. Technol.* **1996**, *4*, 863.

(18) (a) Bakowies, D.; Thiel, W. *Chem. Phys.* **1991**, *151*, 309. (b) Bakowies, D.; Thiel, W. *J. Am. Chem. Soc.* **1991**, *113*, 3704. (c) Cyvin, S. J.; Brendsdai, E.; Brunvoll, J.; Skaret, M. *THEOCHEM* **1991**, *247*, 119. (d) Matsuzawa, N.; Dixon, D. A. *J. Phys. Chem.* **1992**, *96*, 6241. (e) Sastry, G. N.; Jemmis, E. D.; Mehta, G.; Shah, S. R. *J. Chem. Soc., Perkin Trans.* **1993**, 1867. (f) Pope, C. J.; Howard, J. B. *J. Phys. Chem.* **1995**, *99*, 4306. (g) Chakrabarti, A.; Anusooya, Y.; Ramasesha, S. *THEOCHEM* **1996**, *361*, 181. (h) Yavari, I.; Taj- Khorshid, E.; Nori-Shargh, D.; Balalaie, S. *THEOCHEM* **1997**, *393*, 163.

(19) (a) Hebard, A. F.; Rosseinsky, M. J.; Haddon, R. C.; Murphy, D. W.; Glarum, S. H.; Palstra, T. T. M.; Ramirez, A. P.; Kortan, A. R. *Nature* **1991**, *350*, 600. (b) Rosseinsky, M. J.; Ramirez, A. P.; Glarum, S. H.; Murphy, D. W.; Haddon, R. C.; Hebard, A. F.; Palstra, T. T. M.; Kortan, A. R.; Zahurak, S. M.; Makhija, A. V. *Phys. Rev. Lett.* **1991**, *66*, 2830.

(20) Tanigaki, K.; Ebbesen, T. W.; Saito, S.; Mizuki, J.; Tsai, J. S.; Kubo, Y.; Kuroshima, S. *Nature* **1991**, *352*, 222.

(21) Palstra, T. T. M.; Zhou, O.; Iwasa, Y.; Sulewski, P. E.; Fleming, R. M.; Zegarski, B. R. *Solid State Commun.* **1995**, *93*, 327.

(22) (a) Varma, C. M.; Zaanen, J.; Raghavachari, K. *Science* **1991**, *254*, 989. (b) Lannoo, M.; Baraff, G. A.; Schlüter, M.; Tomanek, D. *Phys. Rev. B* **1991**, *44*, 12106. (c) Asai, Y.; Kawaguchi, Y. *Phys. Rev. B* **1992**, *46*, 1265. (d) Faulhaber, J. C. R.; Ko, D. Y. K.; Briddon, P. R. *Phys. Rev. B* **1993**, *48*, 661. (e) Antropov, V. P.; Gunnarsson, O.; Lichtenstein, A. I. *Phys. Rev. B* **1993**, *48*, 7651. (f) Gunnarsson, O. *Phys. Rev. B* **1995**, *51*, 3493. (g) Gunnarsson, O.; Handschuh, H.; Bechthold, P. S.; Kessler, B.; Ganteför, G.; Eberhardt, W. *Phys. Rev. Lett.* **1995**, *74*, 1875. (h) Dunn, J. L.; Bates, C. A. *Phys. Rev. B* **1995**, *52*, 5996. (i) Gunnarsson, O. *Rev. Mod. Phys.* **1997**, *69*, 575. (j) Devos, A.; Lannoo, M. *Phys. Rev. B* **1998**, *58*, 8236. (k) Gunnarsson, O. *Nature* **2000**, *408*, 528.

(23) (a) Kato, T.; Yamabe, T. *J. Chem. Phys.* **2001**, *115*, 8592. (b) Kato, T.; Yamabe, T. *J. Chem. Phys.* **2004**, *120*, 3311. (c) Kato, T.; Yamabe, T. *Recent Research Developments in Quantum Chemistry*; Transworld Research Network: Kerala, 2004. (d) Kato, T.; Yamabe, T. *Recent Research Developments in Physical Chemistry*; Transworld Research Network: Kerala, 2004. (e) Kato, T.; Yamabe, T. *Chem. Phys. Lett.* **2005**, *403*, 113. (f) Kato, T.; Yamabe, T. *Chem. Phys.*, revised.

(24) (a) Coropceanu, V.; Filho, D. A. da Silva; Gruhn, N. E.; Bill, T. G.; Brédas, J. L. *Phys. Rev. Lett.* **2002**, *89*, 275503. (b) Brédas, J. L.; Beljonne, D.; Coropceanu, V.; Cornil, J. *Chem. Rev.* **2004**, *104*, 4971.

(25) Conwell, E. M. *Phys. Rev. B* **1980**, *22*, 1761.

(26) (a) Becke, A. D. *Phys. Rev. A* **1988**, *38*, 3098. (b) Becke, A. D. *J. Chem. Phys.* **1993**, *98*, 5648.

(27) Lee, C.; Yang, W.; Parr, R. G. *Phys. Rev. B* **1988**, *37*, 785.

(28) (a) Ditchfield, R.; Hehre, W. J.; Pople, J. A. *J. Chem. Phys.* **1971**, *54*, 724. (b) Hariharan, P. C.; Pople, J. A. *Theor. Chim. Acta* **1973**, *28*, 213.

(29) Frisch, M. J.; Trucks, G. W.; Schlegel, H. B.; Scuseria, G. E.; Robb, M. A.; Cheeseman, J. R.; Zakrzewski, V. G.; Montgomery, J. A., Jr.; Stratmann, R. E.; Burant, J. C.; Dapprich, S.; Millam, J. M.; Daniels, A. D.; Kudin, K. N.; Strain, M. C.; Farkas, O.; Tomasi, J.; Barone, V.; Cossi, M.; Cammi, R.; Mennucci, B.; Pomelli, C.; Adamo, C.; Clifford, S.; Ochterski, J.; Petersson, G. A.; Ayala, P. Y.; Cui, Q.; Morokuma, K.; Malick, D. K.; Rabuck, A. D.; Raghavachari, K.; Foresman, J. B.; Cioslowski, J.; Ortiz, J. V.; Stefanov, B. B.; Liu, G.; Liashenko, A.; Piskorz, P.; Komaromi, I.; Gomperts, R.; Martin, R. L.; Fox, D. J.; Keith, T.; Al-Laham, M. A.; Peng, C. Y.; Nanayakkara, A.; Gonzalez, C.; Challacombe, M.; Gill, P. M. W.; Johnson, B. G.; Chen, W.; Wong, M. W.; Andres, J. L.; Head-Gordon, M.; Replogle, E. S.; Pople, J. A. *Gaussian 98*, revision x.x; Gaussian, Inc.: Pittsburgh, PA, 1998.

(30) Tanaka, K.; Huang, Y.; Yamabe, T. *Phys. Rev. B* **1995**, *51*, 12715.

(31) Christides, C.; Neumann, D. A.; Prassides, K.; Copley, J. R. D.; Rush, J. J.; Rosseinsky, M. J.; Murphy, D. W.; Haddon, R. C. *Phys. Rev. B* **1992**, *46*, 12088.

(32) Fischer, J. E.; Heiney, P. A.; Smith, A. B. *Acc. Chem. Res.* **1992**, *25*, 112.

(33) Janata; J.; Gendell, J.; Ling, C.-Y.; Barth, W.; Backes, L.; Mark, H. B.; Lawton, R. G. *J. Am. Chem. Soc.* **1967**, *89*, 3056.

(34) Yamabe, T. *Conjugated Polymers and Related Materials*; Oxford University Press: Oxford, U.K., 1993; p. 443.

(35) Kivelson, S.; Heeger, A. J. *Synth. Met.* **1988**, *22*, 371.

(36) McMillan, W. L. *Phys. Rev.* **1968**, *167*, 331.

(37) Hannary, N. B.; Geballe, T. H.; Matthias, B. T.; Andress, K.; Schmidt, P.; MacNair, D. *Phys. Rev. Lett.* **1965**, *14*, 225.

(38) Belash, I. T.; Bronnikov, A. D.; Zharikov, O. V.; Palnichenko, A. V. *Synth. Met.* **1990**, *36*, 283.

(39) Avdeev, V. V.; Zharikov, O. V.; Nalimova, V. A.; Palnichenko, A. V.; Semenenko, K. N. *Pis'ma Zh. Eksp. Teor. Fiz.* **1986**, *43*, 376.

(40) Clarke, R.; Uher, C. *Adv. Phys.* **1984**, *33*, 469.

(41) Haddon, R. C. *Acc. Chem. Res.* **1992**, *25*, 127.

(42) (a) Eliashberg, G. M. *Zh. Eksp. Teor. Fiz.* **1960**, *38*, 966. (b) Eliashberg, G. M. *Zh. Eksp. Teor. Fiz.* **1960**, *39*, 1437. (c) Eliashberg, G. M. *Sov. Phys. JETP* **1960**, *11*, 696. (d) Eliashberg, G. M. *Sov. Phys. JETP* **1961**, *12*, 1000.

(43) Manini N.; Tosatti, E. *Phys. Rev. B* **1998**, *58*, 782.

(44) O'Brien, M. C. M. *Phys. Rev. B* **1996**, *53*, 3775.